Development 136, 551-561 (2009) doi:10.1242/dev.031104

Glycosphingolipids control the extracellular gradient of the *Drosophila* EGFR ligand Gurken

Sandrine Pizette[1,*], Catherine Rabouille[2], Stephen M. Cohen[3] and Pascal Thérond[1]

Glycosphingolipids (GSLs) are present in all eukaryotic membranes and are implicated in neuropathologies and tumor progression in humans. Nevertheless, their in vivo functions remain poorly understood in vertebrates, partly owing to redundancy in the enzymes elongating their sugar chains. In *Drosophila*, a single GSL biosynthetic pathway is present that relies on the activity of the Egghead and Brainiac glycosyltransferases. Mutations in these two enzymes abolish GSL elongation and yield oogenesis defects, providing a unique model system in which to study GSL roles in signaling in vivo. Here, we use *egghead* and *brainiac* mutants to show that GSLs are necessary for full activation of the EGFR pathway during oogenesis in a time-dependent manner. In contrast to results from in vitro studies, we find that GSLs are required in cells producing the TGFα-like ligand Gurken, but not in EGFR-expressing cells. Strikingly, we find that GSLs are not essential for Gurken trafficking and secretion. However, we characterize for the first time the extracellular Gurken gradient and show that GSLs affect its formation by controlling Gurken planar transport in the extracellular space. This work presents the first in vivo evidence that GSLs act in trans to regulate the EGFR pathway and shows that extracellular EGFR ligand distribution is tightly controlled by GSLs. Our study assigns a novel role for GSLs in morphogen diffusion, possibly through regulation of their conformation.

KEY WORDS: Glycosphingolipids, Glycosyltransferases, Egghead, Brainiac, Signaling, Gradient, EGFR, Gurken, Oogenesis, *Drosophila*

INTRODUCTION

Glycosphingolipids (GSLs) are ubiquitous components of eukaryotic cell membranes. They consist of a variable oligosaccharide chain attached to a ceramide lipid backbone (Cer) that tethers them to the lumenal leaflet of membranes. GSLs are mainly synthesized from Cer in the Golgi apparatus by a stepwise process in which unique glycosyltransferases add monosaccharides to a growing lipid-linked oligosaccharide chain. They are subsequently exported towards the plasma membrane, their principal location, where they are enriched together with cholesterol in membrane microdomains. The expression of a particular GSL is differentially regulated according to the developmental stage, the cell type and its differentiation state. The role of vertebrate GSLs has mostly been addressed in vitro (reviewed by Degroote et al., 2004; Sillence and Platt, 2004). These studies indicate that cell-surface GSLs participate in adhesion through the binding in trans of lectins or other GSLs. GSLs can also bind in cis to directly modulate the activity of receptor tyrosine kinases (RTKs) at the plasma membrane. GSLs are also thought to be involved in vesicular transport along the exocytic and endocytic pathways, sorting proteins into different compartments. Lastly, the presence of GSLs in membrane microdomains, which are considered as signaling platforms, may underlie many of their functions.

There is, however, little in vivo evidence to support any of these presumed functions. In *S. cerevisiae*, mutants abolishing all GSL synthesis fail to show defects in intracellular trafficking (Lisman et al., 2004). In *C. elegans*, GSLs appear to be dispensable throughout life (Griffitts et al., 2005). In mammals, the vast majority of GSLs are built on glucosylceramide (GlcCer), and synthesis branches at the level of the third glycosyl residue to yield three classes (lacto-, globo- and ganglioseries, Fig. 1A). Knockout of the mouse GlcCer synthase gene (*Ugcg*) leads to early embryonic lethality, for unclear reasons; assessing the effects of knocking out downstream glycosyltransferases is complicated by redundancy in these genes and between different GSLs (reviewed by Sabourdy et al., 2008). Nonetheless, disrupting the ganglioseries pathway produces mice that display neurological abnormalities after birth. Interestingly, in humans, mutations affecting GSL synthesis and degradation trigger severe neuropathologies (reviewed by Kolter and Sandhoff, 2006). Therefore, GSLs are at least required for proper function of the adult nervous system, but no firm link has yet been established between this requirement and their proposed cellular roles.

Drosophila melanogaster GSLs are simpler in structure than their vertebrate counterparts, with a single biosynthetic pathway described to date, giving rise to a family of differentially elongated molecules (Seppo et al., 2000). We previously identified Egghead (Egh) and Brainiac (Brn) as glycosyltransferases responsible for GSL biosynthesis in the fly, catalyzing the addition of the second and third glycosyl residues of the GSL oligosaccharide chain (Fig. 1B) (Schwientek et al., 2002; Wandall et al., 2003; Wandall et al., 2005). We also showed that there is no redundancy in these enzyme functions and no alternate biosynthetic pathway. Hence, *egh* and *brn* mutants are devoid of elongated GSLs and provide a useful model system for studies of GSL functions in vivo. Importantly, mutations in each gene are lethal and cause identical phenotypes during oogenesis and embryogenesis that are reminiscent of loss-of-function in the Notch receptor and EGF RTK (EGFR) pathways (Goode et al., 1996a; Goode et al., 1996b). Since the expression of a GSL-dedicated human galactosyltransferase in *Drosophila egh* mutants rescues their viability and fertility in a *brn*-dependent fashion (Wandall et al., 2005), these data indicate that *Drosophila* GSLs are essential for development, perhaps by modulating signaling.

[1]Institute of Developmental Biology and Cancer, CNRS UMR 6543, Centre de Biochimie, Université de Nice, Parc Valrose, 06108 Nice Cedex 02, France. [2]The Cell Microscopy Centre, Department of Cell Biology, Institute of Biomembranes, University Medical Centre Utrecht, AZU Room H02.313, Heidelberglaan 100, 3584 CX Utrecht, The Netherlands. [3]Temasek Life Sciences Laboratory, 1 Research Link, Singapore 117604, Republic of Singapore.

*Author for correspondence (e-mail: pizette@unice.fr)

Accepted 2 December 2008

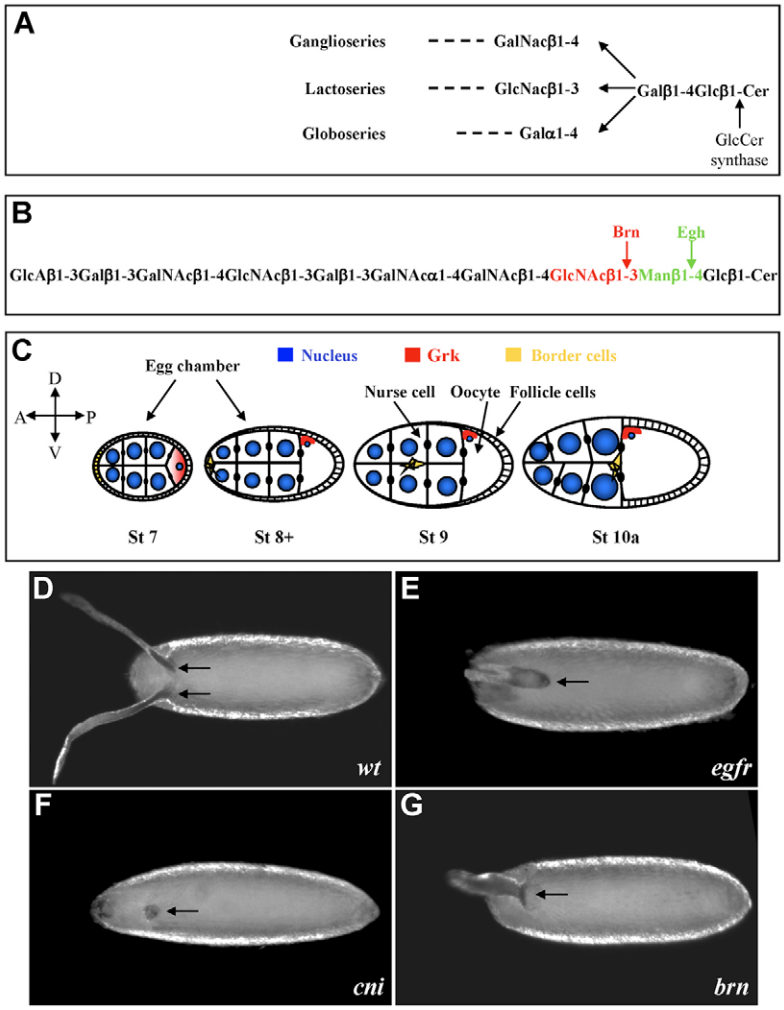

Fig. 1. GSL biosynthetic pathway and establishment of DV polarity during oogenesis. (**A**,**B**) Glycosphingolipid (GSL) biosynthetic pathway in mammals (A) and *Drosophila* (B). Glycan chain biosynthesis proceeds from right to left. (A) Mammalian GSLs are classified into three groups, ganglio-, lacto- and globoseries, depending on which glycosyl residue is added to the invariant diglycosylceramide core. These different triglycosylceramides can be further elongated by glycosyl residues and/or modified by sialic acid (not represented here). (B) Simplified version of the longest *Drosophila* GSL species isolated to date. All other characterized species correspond to shorter forms of this GSL. Egh catalyzes the addition of the second glycosyl residue (a mannose), whereas Brn catalyzes the addition of the third (an N-acetylglucosamine), providing the biosynthetic intermediates for further elongated GSLs. (**C**) Schematics highlighting the events taking place during DV patterning in *Drosophila* ovaries. See text for details. (**D-G**) Dorsal view of *Drosophila* eggs; anterior is to the left. In wild-type (wt) eggs (D), two separate respiratory appendages (RAs) of dorsolateral origin are seen at the anterior side of the egg (arrows). In mutants affecting DV polarity, these structures are either fused, such as in a hypomorphic *Egfr* allele and in a *brn* allele (arrow in E and G, respectively), or missing, such as in a strong hypomorphic combination of *cni* alleles that severely compromises Grk secretion (F, arrow points to a knob of residual appendage material).

During *Drosophila* oogenesis, activation of the EGFR pathway primarily depends on Gurken (Grk), an EGFR ligand similar to vertebrate TGFα, that is secreted by the oocyte (reviewed by Nilson and Schupbach, 1999). The EGFR-Grk couple acts twice to polarize the follicular epithelium as well as the future embryo along both anteroposterior (AP) and dorsoventral (DV) axes (Gonzalez-Reyes et al., 1995; Roth et al., 1995). Despite ubiquitous expression of EGFR in follicle cells, its activation is spatially restricted by asymmetric Grk localization. In early oogenesis, *grk* mRNA and protein are enriched at the posterior pole of the oocyte (Fig. 1C), and Grk activates EGFR in neighboring follicle cells, inducing them to adopt a posterior fate. At mid-oogenesis, these cells signal back to the oocyte, resulting in a reorganization of its cytoskeleton, a redistribution of oocyte maternal determinants along the AP axis, and the movement of the nucleus towards the anterior oocyte cortex. As *grk* RNA remains associated with the oocyte nucleus, a new restricted source of Grk is created to limit the highest activation of EGFR to the adjacent follicle cells, instructing them to assume a dorsal identity (Fig. 1C) (Schupbach, 1987; Neuman-Silberberg and Schupbach, 1993). Respiratory appendages (Fig. 1D) are eggshell structures derived from dorsolateral follicular cells and their examination is an excellent means to monitor EGFR signaling. Indeed, mild Grk or EGFR loss-of-function causes a fusion of the respiratory appendages owing to the absence of the dorsal-most cells (weak ventralization, Fig. 1E). By contrast, a more severe reduction in EGFR signaling abrogates the formation of these structures (complete ventralization, Fig. 1F).

Here, we address the role of GSLs in EGFR signaling during oogenesis using *egh* and *brn* mutants. First, we show that GSLs exert a temporal control on the level of activation of EGFR. We find no evidence of a role for GSLs in the direct modulation of EGFR activity, but instead we show that GSLs act at the level of the EGFR ligand Grk. Despite reports of GSL function in trafficking, our results indicate that GSLs are dispensable for Grk export to the plasma membrane and for its secretion. However, by observing, for the first time, the gradient of secreted Grk, we show that GSLs control Grk diffusion in the extracellular space.

MATERIALS AND METHODS

Fly strains

Flies were raised on standard medium at 25°C, or at 18°C for crosses involving the cold-sensitive brn^{fs107} allele (Goode et al., 1992). Other mutant alleles were: $brn^{1.6P6}$ (Goode et al., 1996b), egh^{62d18}, molecularly characterized by Wandall et al. (Wandall et al., 2005), the top^{1} allele of *Egfr* (Clifford and Schupbach, 1994), cni^{AA12} and cni^{AR55} (Roth et al., 1995) and grk^{DC} (Queenan et al., 1999). GAL4 and UAS lines used: *nos-GAL4* (Rorth, 1998), *e22c-GAL4* (Duffy et al., 1998), *UASP-brn* (Chen et al., 2007) and $UASP\text{-}mbgrk^{myc}$ (Ghiglione et al., 2002), which we remobilized to the third chromosome. $brn^{1.6P6}$ and egh^{62d18} were recombined to *FRT101*, germ line

clones generated with the *hsFLP ovo^{D1}* system (Chou and Perrimon, 1992), and follicle cell clones obtained using the *e22c-GAL4,UAS-FLP* stock (Bloomington Stock Center).

The *brn^{fs107}* allele was characterized by isolating genomic DNA from adult homozygous mutant flies, amplification by PCR of the full *brn* coding sequence and sequencing. Mutations were confirmed in two independent PCR reactions. Cloning details and primer sequences are available upon request.

In situ hybridization, electron microscopy and immunostaining

Whole-mount in situ hybridization for *grk* on ovaries was carried out as described (Vanzo and Ephrussi, 2002). For *rho1* and *aos* mRNAs, amplification was skipped and Fast Red (Roche) was used as a fluorescent substrate for the alkaline phosphatase. Probes were prepared according to the manufacturer's instructions (DIG RNA Labeling Kit, Roche).

Localization of Grk by immunoelectron microscopy was performed as described (Herpers and Rabouille, 2004). Conventional immunostaining was as described (Wandall et al., 2005). Primary antibodies used: mouse monoclonal anti-MacCer (Wandall et al., 2005) undiluted, mouse monoclonal anti-Grk (1D12, DSHB) 1:200, rat polyclonal anti-EGFR (a kind gift from B. Shilo, Weizmann Institute of Science, Rehovot, Israel) 1:100. Fluorescently conjugated secondary antibodies were from Jackson ImmunoResearch. DAPI (Sigma) and fluorescently conjugated phalloidin (Molecular Probes) were always included in the staining procedure. Note that for MacCer staining, we used, as a detergent, Tween 20 at 0.05% instead of Triton X-100 at 0.1%. Extracellular immunostaining was as reported (Strigini and Cohen, 2000).

Confocal data were acquired with a Leica TCS microscope as single images collected from the focal plane in which the oocyte nucleus is visible, or as image stacks for dorsal views.

Characterization of the extracellular Grk gradient

To compare specimens of different genotypes, egg chambers were stained in parallel and imaged with identical acquisition settings. The extent of extracellular Grk diffusion towards the posterior pole was expressed as a ratio of the length of Grk staining in the extracellular space (delimited by F-actin staining) over the total length of the extracellular space along the AP axis (anterior- and posterior-most points were at the boundary with nurse cells and posterior polar follicle cells, respectively). These distances were measured using the Freehand tool from ImageJ, on single images of the longest longitudinal section taken at the level of the dorsal midline.

For dorsal views of the extracellular Grk gradient, quantification of pixel intensity at a defined level was performed with ImageJ on projections of 1 μm-spaced confocal sections encompassing the whole domain of detectable Grk expression (typically ~35 sections, roughly corresponding to the dorsal half of the egg chamber circumference). Average plots from the number of samples indicated in the text were generated using Microsoft Excel.

Western blot

Ovarian extracts were prepared as described (Ghiglione et al., 2002). The rabbit anti-Myc (A-14, Santa Cruz) antibody was used at 1:1000, the mouse monoclonal anti-α-Tubulin (DM 1A, Sigma) at 1:10,000 and HRP-conjugated secondary antibodies (Jackson ImmunoResearch) at 1:5000. Western blots were developed with ECL reagents (Amersham).

RESULTS

GSLs control EGFR activity in the ovarian follicular epithelium

Most mutations in the glycosyltransferases Egh and Brn lead to lethality, or to female sterility when germ line clones are generated, owing to a block in early oogenesis related to the formation of compound egg chambers (egg chambers containing multiple oocyte-nurse cell complexes, see Fig. 1C and asterisk in Fig. 3B) (Goode et al., 1996a; Goode et al., 1996b). As a result, very few eggs are laid, and those that are exhibit weakly ventralized eggshells, suggesting a defect in EGFR activity during DV patterning of the follicular epithelium.

To examine the requirement for GSLs in EGFR signaling, we used the viable and cold-sensitive *brn^{fs107}* allele, in addition to the lethal *egh* and *brn* alleles. We molecularly characterized *brn^{fs107}* and found a single nucleotide substitution changing the conserved tyrosine residue at position 147 to an asparagine. Even when raised at 18°C, *brn^{fs107}* mutant females are fertile and rarely display early oogenesis defects, but produce eggs with fused respiratory appendages (RAs) (Fig. 1G, arrow). At this temperature, the *brn^{fs107}* eggshell phenotype is highly penetrant and this allele behaves genetically as a null for this phenotype (Goode et al., 1992). Because of its viability and robust eggshell defect, the *brn^{fs107}* allele is useful to study the role of GSLs in late oogenesis events such as DV patterning.

To assess the level of EGFR activity in the follicular epithelium of the *brn^{fs107}* mutant during DV patterning, we looked at the expression of *argos* (*aos*), which requires amplification of EGFR signaling, and of *rhomboid1* (*rho1*; *rho* – FlyBase), which is induced prior to the amplification phase (Wasserman and Freeman, 1998). In wild-type stage 11 egg chambers, *aos* mRNA is expressed in follicle cells in a triangle above the oocyte nucleus, being more abundant at the anterior margin of the epithelium (Fig. 2A,A′, arrow). *rho1* transcripts are present as two L-shaped stripes, in a pattern complementary to that of *aos* (Fig. 2C,C′). In stage 11 *brn* mutants, *aos* and *rho1* were still expressed, but at lower levels. *aos* mRNA was only detected in the anterior-most follicle cells (Fig. 2B,B′, arrow), whereas *rho1* transcripts were distributed in a single broad domain covering the anterior third of the dorsal follicular epithelium (Fig. 2D,D′, bracket). Strikingly, these expression domains resemble the wild-type *aos* and *rho1* patterns from stage 10a egg chambers (see Peri et al., 1999; Queenan et al., 1997; Ruohola-Baker et al., 1993). This suggests that

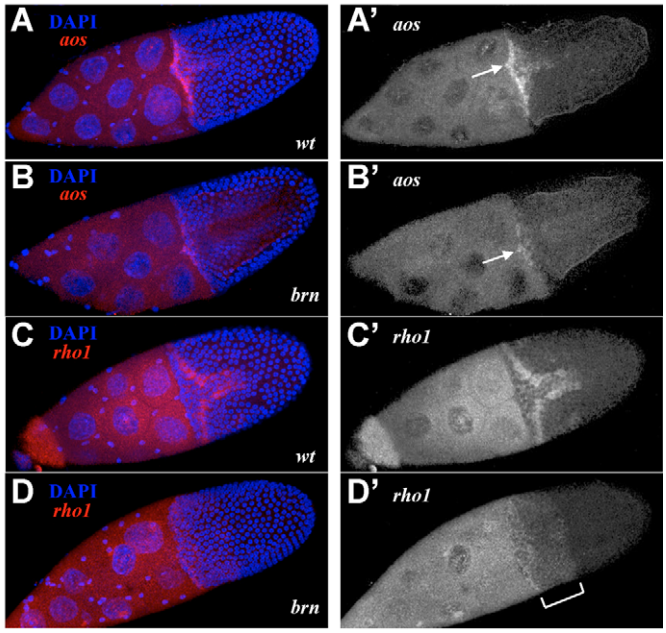

Fig. 2. GSLs are needed for full activation of the EGFR pathway. (**A-D′**) Stacks of confocal images showing dorsal views (anterior is left) of stage 11 *Drosophila* egg chambers processed for RNA in situ hybridization with an *argos* probe (*aos*, red in A,B, shown alone in A′,B′) or a *rhomboid1* probe (*rho1*, red in C,D, shown alone in C′,D′). In wild-type samples (A,C), *aos* is expressed in dorso-anterior (DA) follicle cells in a triangle (arrow in A′) and *rho1* transcripts are enriched in two L-shaped stripes (C′). In *brn* mutant samples (B,D), *aos* expression is almost extinguished (arrow in B′), whereas low-level, rather uniform *rho1* expression remains (bracket in D′).

the initial activation of EGFR by Grk proceeded normally, but that the amplification process itself did not take place. These observations fit nicely with the fusion of the RA in the *brn* mutant because the amplification step and *aos* expression are necessary for the splitting of the RA (Wasserman and Freeman, 1998). These results provide evidence that GSLs are required during DV patterning of the follicle cells to achieve high levels of EGFR activity.

GSLs are required in the germ line for EGFR activity in follicle cells

A decrease in EGFR signaling could originate from a defect at any level of the pathway. Cell culture studies have shown that vertebrate GSLs physically interact with EGFR, modulating its activity in cis (Miljan et al., 2002; Yoon et al., 2006). Given that the GSL biosynthetic pathway is active in the follicular epithelium (Wandall et al., 2005), we might expect GSLs to be required in follicle cells. Nonetheless, clonal analysis has suggested that *egh* and *brn* are required in the germ line (Goode et al., 1996a). It is thus possible that GSLs act in both tissues.

To investigate this, we extended our previous analysis of the activity of the GSL biosynthetic pathway during oogenesis. Since antibodies against elongated GSLs or Egh and Brn are not available, we used an antibody that specifically recognizes the non-elongated biosynthetic intermediate produced by Egh, mactosylceramide (MacCer, Fig. 3A) (Wandall et al., 2005). Theoretically, MacCer detection indicates that Egh is active. However, MacCer staining was never seen in wild-type ovaries (Wandall et al., 2005) (data not shown), suggesting (1) that Egh is not expressed in this tissue or (2) that Egh is expressed but that Brn immediately elongates MacCer. In the second case, abrogating *brn* function should lead to MacCer accumulation. When we examined MacCer distribution in brn^{fs107} ovaries (Fig. 3B and data not shown), we found MacCer staining in the germarium (the structure producing the egg chambers) and early egg chambers. MacCer was again detected at stage 8, when DV patterning of the follicular epithelium is initiated, and persisted at least until stage 11. MacCer was present in follicle cells, confirming our previous observations, but was also strongly detected in both nurse cells and oocyte. This pattern is not allele-specific, as $brn^{1.6P6}$ follicle cell and germ line clones generated at different time points gave the same result (data not shown). Therefore, the GSL pathway is active in both germ line and somatic follicle cells at the time when DV patterning is being established.

Next, we tested whether GSLs from follicle cells or the germ line participate in EGFR signaling. We produced egg chambers with large clones of follicle cells mutant for the lethal alleles $brn^{1.6P6}$ or egh^{62d18}, without affecting the germ line. In these experiments, the percentage of mutant follicular epithelia was high (65.8% for $brn^{1.6P6}$ as determined by MacCer staining; n=38 stage 10 and 11 egg chambers; data not shown), yet none of the eggs derived from such chambers exhibited defects in the DV polarity of their eggshells (Table 1A). In agreement with Goode and colleagues (Goode et al., 1996a), germ line clones of these alleles led to the formation of eggs with fused RAs (Table 1B). Furthermore, restricted expression of a *UAS-brn* transgene to the oocyte of brn^{fs107} mutants completely rescued the ventralized eggshell phenotype (Table 1C). Altogether, these results indicate that GSLs are required in the germ line, but not in follicle cells, to support EGFR activity in follicle cells. This suggests a role in the ligand-producing cell, arguing against a direct modulation of EGFR activity in cis in this context.

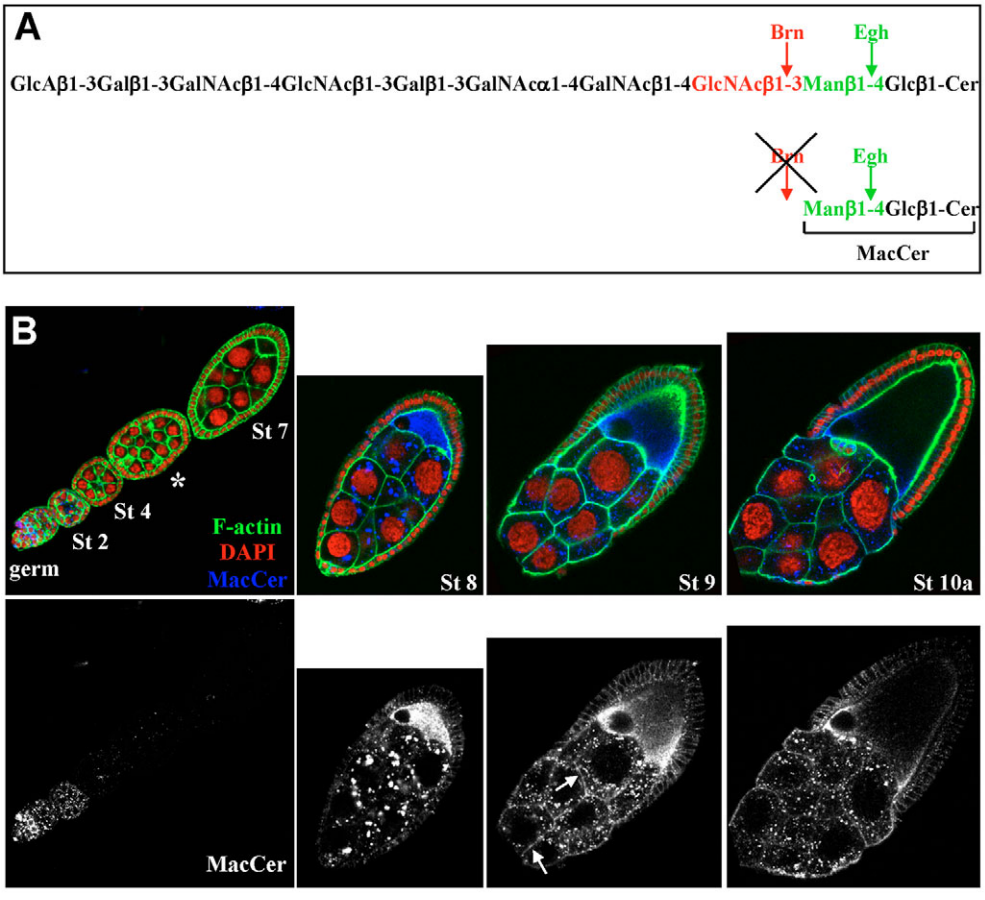

Fig. 3. The GSL biosynthetic pathway is active in both germ line and follicle cells. (**A**) Upon loss of *brn* function, the intermediate product mactosylceramide (MacCer), synthesized by Egh, cannot be extended and accumulates. This product is specifically recognized by our antibody. (**B**) Confocal images of *brn* homozygous mutant *Drosophila* egg chambers of the indicated stages stained with anti-MacCer antibody (blue). The asterisk marks an egg chamber that could not be staged because it is compound. MacCer staining (shown alone in the bottom row of panels) is detected in the germarium (germ) and in newly budded egg chambers. Expression disappears between stages 4 and 7. From stage 8 onward, MacCer staining is present at the membrane of follicle cells. It is also observed in nurse cells at their membranes (arrows), but mostly in intracellular aggregates. In oocytes, MacCer staining is uniform at stage 8 and shifts towards the anterior cortex between stages 9 and 10 to remain strong in the vicinity of the nucleus. Wild-type egg chambers are negative for MacCer staining (not shown). Anterior is to the left and dorsal is up.

Table 1. GSLs from the germ line are necessary for EGFR signaling

A

Genotype	Phenotype (%)		
	Complete fusion	Partial fusion	Wild type
brn$^{1.6P6}$*FRT101;e22cGAL4FLP* (*n*=500)	0.2±0.4	0.6±0.9	99.2±0.8
egh^{62d18}*FRT101;e22cGAL4FLP* (*n*=500)	0±0	1.6±1.1	98.4±1.1

B

Genotype	Phenotype (%)	
	Complete or partial fusion	Wild type
brn$^{1.6P6}$*FRT101/Ovo*^{D}*FRT101;hsFLP* (*n*=213)	34.3	65.7
egh^{62d18}*FRT101/Ovo*^{D}*FRT101;hsFLP* (*n*=87)	42.5	57.5

C

Genotype	Phenotype (%)		
	Complete fusion	Partial fusion	Wild type
brn^{fs107} (*n*=300)	83.9±9.2	14.9±8.1	1.2±1.4
brn^{fs107}*;;nosGAL4/UASPbrn* (*n*=300)	0±0	0.7±0.6	99.3±0.6

Follicle cell (A) and germ line (B) clones were generated for a lethal allele of *egh* or *brn*. Only eggs derived from germ line clones show a fusion of their RAs. Note that in B, the s.d. is not included because females from these genotypes laid very few eggs, precluding statistical analysis. (C) The appendage fusion phenotype of the *brn* viable allele is rescued by *brn* expression in the germ line.

GSLs regulate Grk distribution

Given the requirement for GSLs in the germ line, we examined whether the distribution of *grk* mRNA or Grk protein would be altered in *brn* mutant oocytes (see Introduction). In stage 10a egg chambers, the localization of *grk* transcripts in *brn*^{fs107} mutant oocytes was indistinguishable from that in the wild type: *grk* mRNA remained in the dorso-anterior (DA) corner, tightly associated with the oocyte nucleus (Fig. 4A,B).

By contrast, we detected stage-specific changes in Grk protein distribution. In wild-type egg chambers at stage 8, Grk was concentrated within the oocyte at its DA corner (Fig. 4C,C′). It was also present at the interface between the oocyte and the follicular epithelium, just above the oocyte nucleus, as a result of directional transport (Herpers and Rabouille, 2004). A small fraction of Grk is seen in adjacent follicle cells, reflecting uptake of secreted Grk (Ghiglione et al., 2002; Peri et al., 1999; Queenan et al., 1999). At stages 10a and 10b, the same pattern as previously was observed (Fig. 4E-G′), but in addition Grk was prominently localized in the extracellular space between the DA corner of the oocyte and the follicular epithelium, in dot-like structures. It was detected there at a considerable distance from the oocyte nucleus, indicative of Grk diffusion from the site of its secretion.

In the *brn* mutant, there was no difference to the wild type at stage 8 (Fig. 4D,D′), but from stage 10a, all *brn* mutant egg chambers displayed abnormal Grk localization (Fig. 4H-I′). Although Grk was still present near the oocyte nucleus, it was noticeably absent from the extracellular space. Moreover, we saw very little evidence of internalized Grk (Fig. 4I′, arrow and arrowheads; data not shown). These findings indicate that GSLs are dispensable for initial Grk secretion at the DA corner at stage 8, but that they are implicated either in sustained Grk secretion or in Grk stabilization once released at stage 10a.

GSLs are not necessary for Grk trafficking to the plasma membrane

To discriminate between sustained secretion or stabilization of Grk, we first sought to determine whether Grk secretion was blocked in stage 10a *brn* mutant egg chambers. Grk is synthesized as a transmembrane molecule that is cleaved in the endoplasmic reticulum (ER) by a member of the Rho family, possibly Rho2 (Stet – FlyBase) (Bokel et al., 2006; Ghiglione et al., 2002; Guichard et al., 2000; Urban et al., 2002). Although this processing is not necessary for Grk trafficking to the plasma membrane, it is a prerequisite for its secretion and activity (Bokel et al., 2006; Ghiglione et al., 2002; Peri et al., 1999; Queenan et al., 1999). The cleaved lumenal portion of Grk is then exported to the Golgi apparatus with the help of its cargo receptor Cornichon (Cni) (Bokel et al., 2006; Roth et al., 1995). Importantly, when either step is compromised, Grk mislocalizes in the oocyte cytoplasm. For instance, an uncleaved Grk accumulates in, and is dispersed throughout, the oocyte cytoplasm (Fig. 5D,D′). In a *cni* mutant, Grk abnormally diffuses into the ER lumen (Fig. 5C,C′).

In *brn* mutant oocytes, however, Grk did not appear to accumulate or mislocalize in the cytoplasm (Fig. 5B,B′), suggesting that its cleavage and export towards the plasma membrane were normal. Nevertheless, Grk could remain unprocessed in *brn* mutants and be rapidly targeted for degradation, preventing its accumulation and mislocalization. To investigate this, we performed a western blot on wild-type and *brn* ovarian extracts. Since endogenous Grk is notoriously difficult to detect by this technique, we overexpressed a construct encoding a Myc-tagged Grk protein in the germ line (Ghiglione et al., 2002). As in the wild type, Grk was still cleaved in the *brn* mutant (Fig. 5E).

To further explore whether Grk follows its normal exocytic route in the *brn* mutant, we compared Grk distribution in stage 10a wild-type and mutant oocytes by immunoelectron microscopy. As previously reported (Herpers and Rabouille, 2004), the bulk of intracellular Grk in wild-type samples was found in tER-Golgi units close to the oocyte nucleus (Fig. 5F). In *brn* mutants, Grk was also detected in these organelles (the morphology of which was normal), where its labeling density was not very different from that in wild-type ovaries (Fig. 5G and data not shown). Moreover, we observed neither an accumulation nor a loss of Grk pre- or post-Golgi (including at the plasma membrane) (data not shown). Altogether, these data argue against an essential role for GSLs in Grk transport to the plasma membrane.

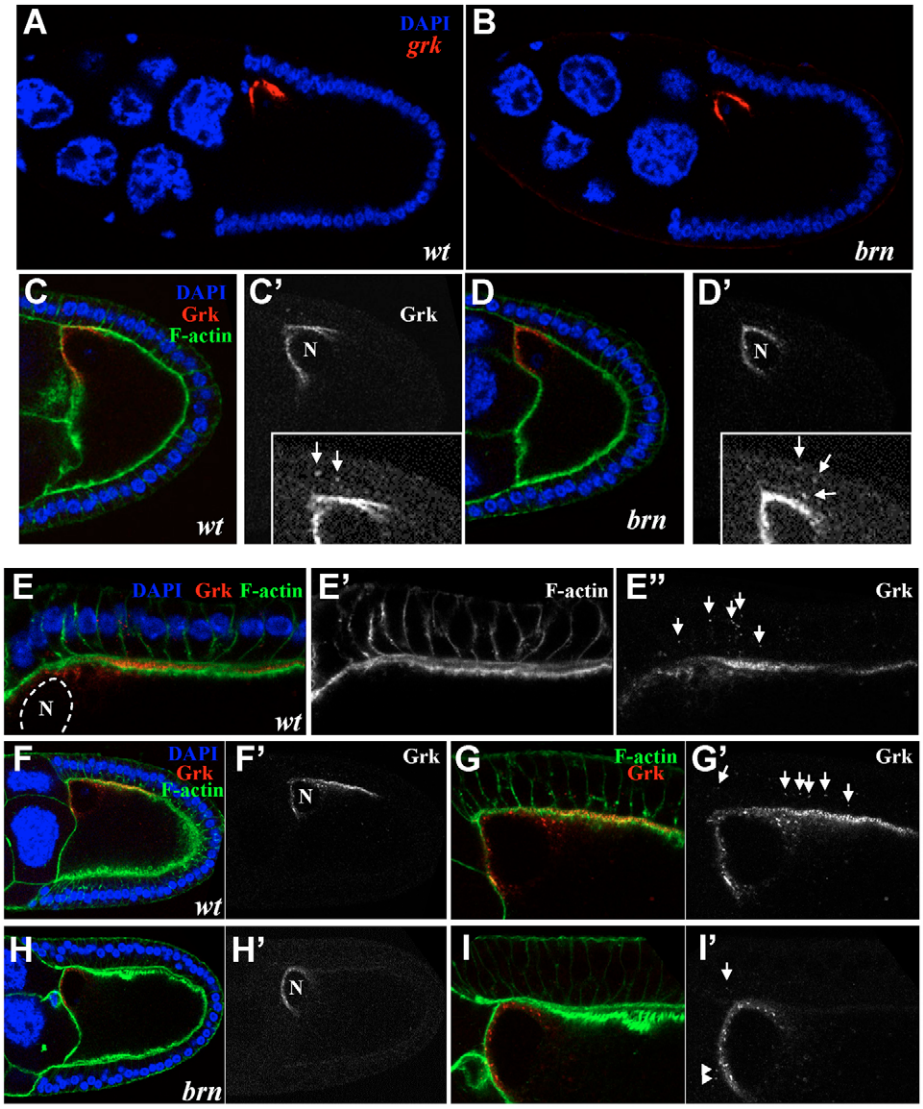

Fig. 4. A stage-specific requirement for GSLs in Grk distribution. (**A**,**B**) Confocal images of stage 10a *Drosophila* egg chambers processed for RNA in situ hybridization with a *grk* probe (red). *grk* mRNA is tightly localized around the nucleus in both wild-type (A) and *brn* mutant (B) oocytes. (**C-I'**) Confocal images of egg chambers labeled by immunofluorescence for Grk protein. (C-D') Stage 8 egg chambers. In both wild-type (C) and *brn* mutant (D) egg chambers, Grk (red, shown alone in C',D') is detected in the cytoplasm and at the cortex of the oocyte (labeled for F-actin, green), in the close vicinity of the nucleus, as well as in adjacent follicle cells (arrows in insets in C',D'). (E-E″) Stage 10b wild-type egg chamber showing an enlargement of the DA region of the oocyte and follicular epithelium. (F-I') Stage 10a egg chambers. G,I show enlargements of the DA region of the oocyte and follicular epithelium from the chambers shown in F,H, respectively. In wild-type specimens (E-G'), Grk (red, shown alone in E″,F',G') is present in the oocyte cytoplasm close to the nucleus, and in neighboring follicle cells (arrows). The bulk of Grk, however, lies in the extracellular space between the cortices of the oocyte and the follicular epithelium (identified by F-actin staining, green, as shown alone in E'). *brn* mutant oocytes (H,I') exhibit levels of Grk (shown alone in H',I') in their cytoplasm that are comparable to those in the wild type. Grk, however, is absent from the extracellular space and is only observed in the anterior-most follicle cells (arrow in I'; compare with the wild type, arrows in G') and in border cells (arrowheads in I'; the border cell cluster in not in the plane of the section in the wild type). Anterior is to the left, dorsal is up. N, oocyte nucleus.

GSLs are not required for Grk to be secreted and functional

These last results suggest that Grk is secreted in the *brn* mutant. To confirm this, we compared the phenotypes resulting from Grk overexpression in wild-type versus *brn* mutant backgrounds (Table 2). Grk overexpression in wild-type oocytes induces a range of gain-of-function phenotypes seen as increasingly dorsalized eggshells (Neuman-Silberberg and Schupbach, 1994). In the *brn* mutant, not only did the eggshells lose their ventralization defect upon Grk overexpression, but they were also dorsalized. This implies that GSLs are not crucial for the secretion of a ligand that is, in addition, functional.

This then raises the question as to why the EGFR pathway is not properly activated in the *brn* mutant. It has been reported that DA follicle cells from stage 10 wild-type egg chambers have a lower amount of EGFR than the rest of the epithelium (Sapir et al., 1998). The authors suggested that in response to EGFR signaling, *Egfr* transcription is downregulated. We therefore used the decrease in EGFR levels as a measure of its activation by Grk.

First, we re-examined EGFR distribution in a wild-type background, as well as in a *cni* mutant as a negative control. As expected, at stage 10a, wild-type egg chambers displayed faint EGFR staining in most follicle cells of the dorsal midline (Fig. 6A,A', arrowheads in A). In *cni* mutants, in which Grk is not secreted, EGFR staining was uniform (Fig. 6B-B″), establishing that its asymmetrical expression is a consequence of its own activation.

We then looked at EGFR distribution in *brn* mutant egg chambers. We found that throughout oogenesis, the EGFR pattern was identical to that observed in wild-type samples (Fig. 6C-C″, arrowheads; data not shown). Our data thus show that in the *brn* mutant, Grk is as active in the maintenance of the spatial regulation of EGFR in DA follicle cells as in wild-type egg chambers. It is however possible that the threshold level of Grk needed to maintain this regulation is lower than that required for proper *rho1* and *aos* expression, and that the role of GSLs is in the regulation of the spatial distribution of secreted Grk.

GSLs shape the extracellular Grk gradient

To examine whether GSLs regulate the spatial distribution of secreted Grk, we visualized, for the first time, the extracellular Grk gradient in stage 10a wild-type and *brn* mutant egg chambers, using conditions that are more sensitive for the detection of extracellular proteins than conventional immunostaining (Strigini and Cohen, 2000). We found that this method is suitable to monitor Grk

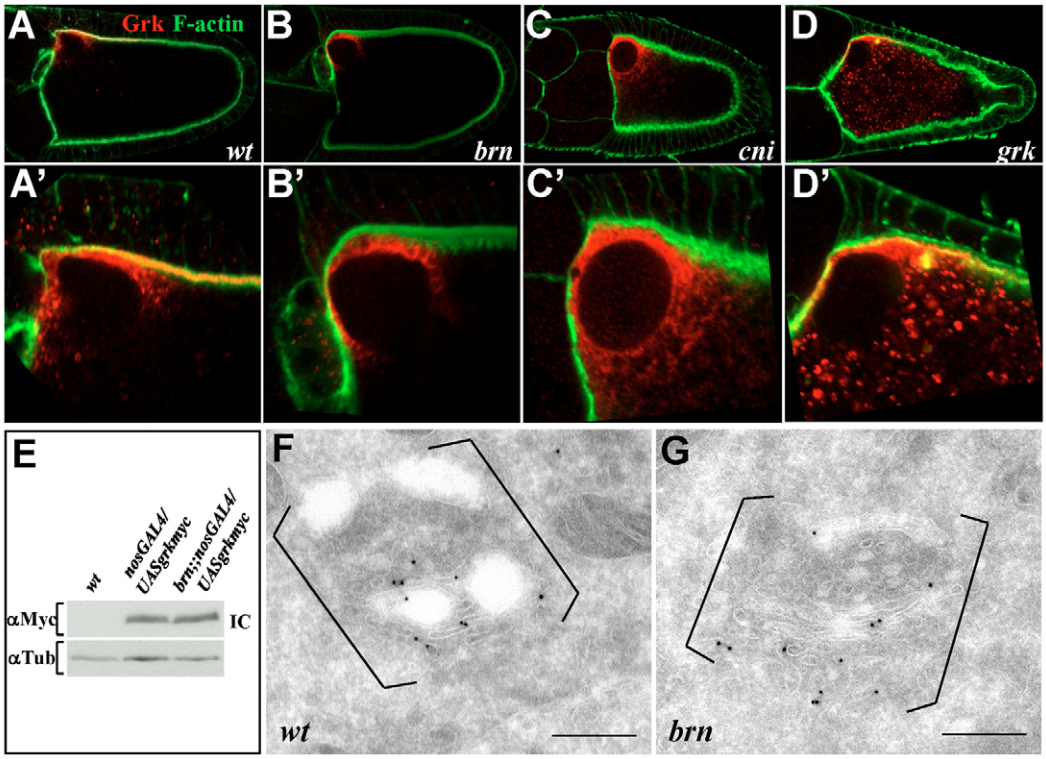

Fig. 5. GSLs are dispensable for Grk trafficking to the plasma membrane. (**A-D'**) Confocal images of stage 10a *Drosophila* egg chambers labeled by immunofluorescence for Grk (red). Enlargements of the DA region of the oocyte and follicular epithelium are shown in A'-D'. Anterior is to the left and dorsal is up. In cni^{AA12}/cni^{AR55} mutant samples (C,C'), Grk is not secreted and localizes neither to the extracellular space separating the oocyte from the follicular epithelium, nor to follicle cells (compare with wild-type sample, A,A'). Instead, it diffuses into the ER lumen of the oocyte, where it is trapped (reticular staining surrounding the nucleus in C'). In samples from the grk^{DC} allele (D,D'), which expresses an uncleavable Grk, Grk is also absent from the extracellular space and from follicle cells, but it reaches the oocyte cortex and it is dispersed throughout the oocyte cytoplasm (yellow staining in D' corresponds to Grk overlapping with the cortex stained for F-actin in green). In *brn* mutant samples (B,B'), despite the lack of Grk in the extracellular space and in most follicle cells, Grk does not mislocalize or accumulate in the oocyte cytoplasm. (**E**) Western blot analysis of Grk cleavage. Extracts from wild-type ovaries, and from wild-type or *brn* mutant ovaries expressing an intracellularly Myc-tagged *grk* construct in their germ line (driven by *nosGAL4*). Tubulin (Tub) was used as a loading control. In both wild-type and *brn* mutant backgrounds, the anti-Myc antibody detects a comparable amount of the cleaved intracellular (IC) portion of Grk, revealing similar cleavage efficiencies. (**F**,**G**) Transmission electron micrographs of the DA region of stage 10a egg chambers. Ultrathin cryosections were immunolabeled for Grk (10 nm, gold). A tER-Golgi unit close to the oocyte nucleus is shown (brackets). The most abundant labeling for Grk in a wild-type (F) or *brn* mutant (G) oocyte is at the tER-Golgi units. Note that the density of this labeling is similar in the two backgrounds. Scale bars: 200 nm.

distribution over the dorsal half of wild-type egg chambers, but the predicted ventral pool (Chang et al., 2008; Goentoro et al., 2006) was below detection.

In wild-type samples (Fig. 7A), the highest levels of extracellular Grk were concentrated within a rectangle-like domain along the dorsal midline. Strikingly, in *brn* samples, extracellular Grk was readily detected and occupied a domain that adopted a triangular shape, with a broad base toward the anterior oocyte cortex (Fig. 7B). We analyzed the Grk gradient in the two backgrounds by measuring the intensity of Grk staining along the DV axis and the dorsal midline.

Along the DV axis at the level of the source (above the oocyte nucleus, Fig. 7C), there was a greater amount of Grk in the *brn* mutant: the maximal intensity was almost double that of the wild type, and intensity values of 80 and above (dashed line) covered a distance approximately twice as long as in the wild type. It should be noted that follicle cells in this area are not fated to become part of the RA (Dorman et al., 2004). This Grk accumulation was restricted to the region overlying the nucleus in the *brn* mutant. Just posterior to this region (Fig. 7D), the maximal intensity was equal to that in the wild type, although it was still maintained over a greater area.

Along the dorsal midline, Grk levels in wild-type egg chambers were steeply elevated posterior to the source (Fig. 7E, asterisk) and reached a plateau, before declining. In *brn* mutants, a plateau of equivalent intensity was also formed, but its length was strongly reduced. In terms of spreading, however, there was still a low amount of Grk (intensity values above 50) that extended as far posteriorly as in the wild type.

The analysis of the extracellular Grk gradient therefore highlighted two major differences in the mutant versus wild-type background: the bulk of Grk diffusion was more efficient along the DV axis at the source and less efficient along the dorsal midline. Since the process that is compromised in the *brn* mutant is the splitting of the RA that requires high-level EGFR signaling to induce *aos* expression at the dorsal midline, these data indicate that GSLs play a crucial role in Grk signaling by preventing its diffusion away from the dorsal midline, thus maintaining high levels of extracellular Grk in this region.

Last, we asked whether EGFR, although seemingly normally distributed (Fig. 6), is involved in the altered diffusion of extracellular Grk in *brn* mutant chambers. To determine how Grk

Table 2. Grk overexpression still induces a gain-of-function phenotype in the absence of elongated GSLs

	Occurrence of the dorsalization phenotype (%)			
	No phenotype	Weak	Medium	Strong
Genotype	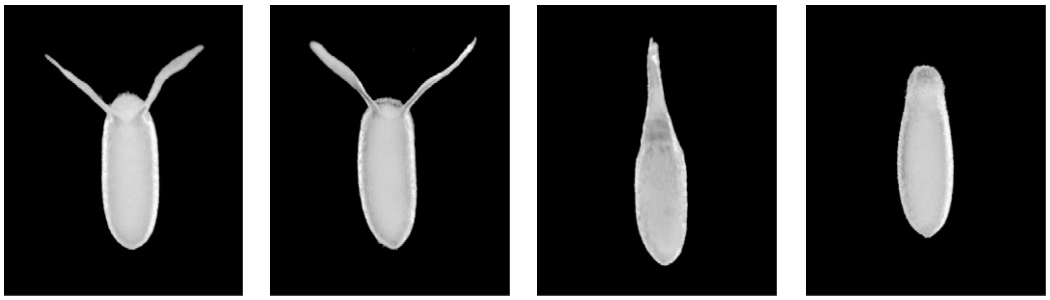			
w;;nosGAL4/UASPmbgrkmyc (*n*=300)	9.7±2	11.3±3.5	56±2	23±1
brn;;nosGAL4/UASPmbgrkmyc (*n*=300)	0±0	0±0	100±0	0±0

Germ line overexpression of *grk* in a wild-type background produces a range of dorsalization phenotypes that can be classified into four groups: 'no phenotype' (i.e. eggs that resemble wild-type); 'weak', which corresponds to eggs that have RAs set further apart; 'medium', in which appendage material surrounds the entire anterior circumference of the egg; and 'strong', in which operculum-like material (anterior dorsal midline fate) occupies the entire anterior circumference of the egg (Queenan et al., 1997). Upon germ line *grk* overexpression in the *brn* mutant background, eggs are dorsalized, indicating that Grk is secreted and active in the absence of GSLs.

binding to its receptor controls its extracellular movement, we used the top^1 allele of *Egfr*. This is a hypomorphic viable allele that bears a point mutation in the ligand-binding domain (Clifford and Schupbach, 1994), causing homozygous females to lay eggs with fused RAs (Fig. 1E). In our hands, this mutant was subviable and we obtained very few top^1 egg chambers of the right stage, all of them oriented in lateral views. This precluded analysis of the Grk gradient in dorsal views, but allowed us to measure extracellular Grk spreading at the dorsal midline in longitudinal confocal sections (Fig. 7F-K′). High and low levels combined, Grk spanned, on average, 69.4 ± 4.2% of the AP length of the extracellular space in top^1 samples (n=7), versus 54.7 ± 3.4% for wild-type samples (n=17). This result demonstrates that EGFR limits the range of extracellular Grk diffusion. By contrast, this value, although slightly reduced, was not significantly different in the *brn* mutant (48 ± 4.6%, n=14), indicating that Grk still efficiently binds EGFR.

In conclusion, our experiments show that GSLs shape the extracellular Grk gradient and strongly suggest that this is achieved through the direct modulation of Grk diffusion.

DISCUSSION

Here, we have assessed the function of GSLs in EGFR signaling during DV patterning of the *Drosophila* egg chamber. In this context, we find no evidence for the reported roles of GSLs in the direct modulation of EGFR activity and in trafficking. Instead, our results show that once Grk is secreted, GSLs are necessary for its efficient diffusion in the extracellular space. Although we cannot dismiss the possibility that GSLs might have a slight influence on Grk secretion, a decrease in Grk secretion cannot explain the observed changes in the extracellular Grk gradient shape in the *brn* mutant or the higher levels of secreted Grk that accumulate above the source, as compared with the wild type. GSLs are thus crucial for the formation of a Grk gradient that is able to achieve maximal activation of EGFR.

Regulation of Grk signaling by GSLs: temporal or spatial?

Surprisingly, we find that GSLs are only involved in the final step of Grk signaling during the establishment of the DV axis. Prior to DV patterning, Grk activates EGFR to set the AP axis of the egg (see Introduction). We have observed, however, that AP polarity is not compromised in *egh* and *brn* alleles (S.P., unpublished). Our analysis of MacCer distribution during oogenesis also supports the idea that the GSL biosynthetic pathway is not active at the time AP patterning is established (Fig. 3). Grk signaling therefore seems to be more sensitive to GSL function for the determination of DV fates.

Even during this process, there appear to be differential requirements for GSL activity. DV patterning proceeds in two distinct temporal phases of EGFR signaling, but only the second is under the control of GSLs. In a first phase (between stages 8 and 10a), the EGFR pathway establishes embryonic DV polarity and dorsal follicle cell fates. This phase culminates in the induction of *rho1* transcription in DA follicle cells and depends on paracrine signaling mediated by Grk. This initial phase is not overtly affected in *brn* mutants as their embryos have a normal DV axis (Goode et al., 1992) and we found that *rho1* expression was still induced (Fig. 2). By contrast, the second phase of EGFR signaling is triggered by *rho1* expression and corresponds to an amplification of EGFR activity needed to split the RA (Wasserman and Freeman, 1998). This phase is disrupted in the *brn* mutant because the expression of *rho1* and *aos* is not upregulated (Fig. 2), as exemplified by the fusion of the RA.

According to Wasserman and Freeman, the amplification phase is independent of Grk and relies on autocrine EGFR signaling (Wasserman and Freeman, 1998). However, we show here that GSLs, unlike the other molecules implicated in this process, act in the germ line to regulate the distribution of extracellular Grk (Table 1 and Fig. 7A-E). This indicates, as previously suggested by others (Peri et al., 1999), that this phase is not solely autocrine and that there is still a need for Grk-mediated paracrine signaling.

At stage 10a, the vitelline membrane is already being deposited as vitelline bodies in the extracellular space between the oocyte and the follicular epithelium. Morphological data show that these bodies have not yet fused, leaving space for a number of interdigitating microvilli emanating from the oocyte membrane and the apical side of the follicle cells (King, 1970). Since the *brn* mutation specifically affects Grk signaling at this stage, we propose that GSLs play a role in Grk accessibility to follicle cells and that this is likely to be mediated through the microvilli. In support of this, at stages at which

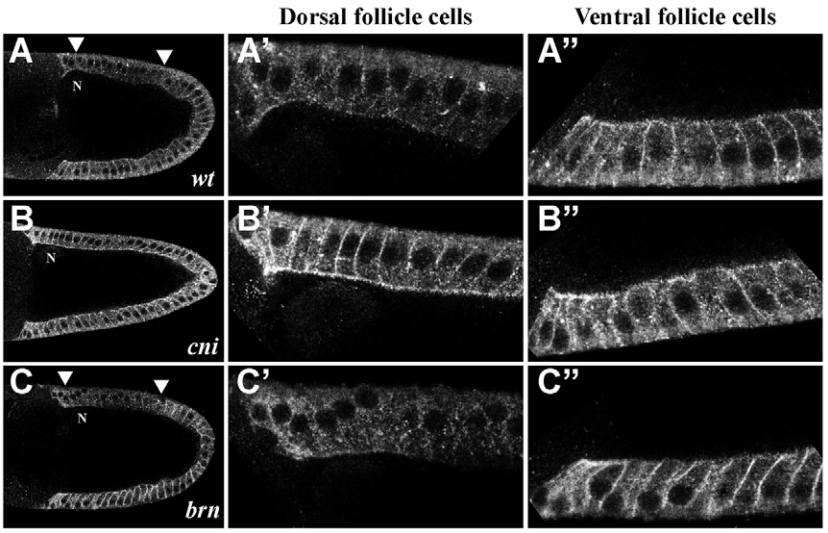

Fig. 6. GSLs are not required for Grk to maintain the spatial regulation of EGFR. Confocal images of stage 10a *Drosophila* egg chambers from the wild type (**A-A″**), and from *cni* (**B-B″**) and *brn* (**C-C″**) mutants, labeled by immunofluorescence for EGFR. Enlargements of the anterodorsal (A′-C′) and the anteroventral (A″-C″) parts of the follicular epithelium are shown. EGFR distribution is asymmetric in wild-type egg chambers (A), the protein being barely detectable (A′) in most of the dorsal midline (region delimited by arrowheads in A), while it is enriched at the apical and lateral membranes of ventral follicles cells (A″). *cni* mutant egg chambers (B), however, display EGFR staining characteristic of ventral follicle cells throughout their epithelium (compare B′ with B″). In *brn* mutant egg chambers (C), EGFR distribution remains asymmetric along the DV axis, with lower protein levels in DA follicle cells (region delimited by arrowheads in C; compare C′ with C″). In all samples, F-actin staining is uniform throughout the follicular epithelium (not shown). Anterior is to the left, dorsal is up. N, oocyte nucleus.

elongated GSLs are not essential (AP patterning and the onset of DV patterning), the oocyte plasma membrane is closely apposed to the apical side of the follicle cells. This, therefore, supports our hypothesis that GSLs are only required when Grk is not easily accessible to its receptor.

An unconventional extracellular Grk gradient

Our study provides the first experimental description of the wild-type extracellular Grk gradient at stage 10a and uncovers an unexpected feature (Fig. 7A,C-E): at the dorsal midline, past the source, high and steady levels of Grk are maintained over about half of the AP axis length. This result is at odds with a mathematical modeling of the Grk gradient that predicted a shallow decrease from anterior to posterior (Goentoro et al., 2006). However, from a strong and constant level of Grk over half the dorsal midline, we expect the expression domains of the Grk primary target genes to have an identical width along most of the AP axis. This is precisely what is observed for *kekkon-1* and *pipe*, which are clearly EGFR primary target genes (Chang et al., 2008; Peri et al., 2002; Sapir et al., 1998; Sen et al., 1998). We thus suggest that a stripe-shaped source of extracellular Grk along the dorsal midline, rather than a point-like source of Grk above the oocyte nucleus, is more efficient in accommodating patterning across the entire epithelium.

Besides contributing to the shape of the Grk gradient, high Grk levels along the dorsal midline might serve to upregulate *rho1* expression, leading to higher EGFR activity, *aos* expression and splitting of the RA primordium. Indeed, we have shown that in the absence of elongated GSLs, weak *rho1* expression is retained but it is not upregulated or refined. As mentioned above, Grk signaling is necessary for this step. Since, in the *brn* mutant, there is a reduction in the high levels of extracellular Grk along the dorsal midline, we propose that a low Grk threshold is sufficient to initiate and maintain *rho1* transcription (as well as the spatial regulation of EGFR, Fig. 6C-C″), whereas a higher Grk threshold increases *rho1* expression levels.

What could be the basis for the discrepancy between our results and the mathematical modeling of the Grk gradient? In the latter (Goentoro et al., 2006), EGFR expression was assumed to be uniform throughout the follicular epithelium. However, we showed that at stage 10a, EGFR levels are lower along part of the dorsal midline (Fig. 7) in a region coincident with that of high Grk levels. Furthermore, we found that decreasing Grk binding to EGFR increased Grk spreading (Fig. 7F-K′). Therefore, at the dorsal midline, the reduction in EGFR levels might saturate receptor occupancy. This could allow a large quantity of Grk to remain unbound, facilitating its movement toward the posterior pole.

Role of GSLs in determining the shape of the extracellular Grk gradient

Our most striking result is that GSLs shape the extracellular Grk gradient and play a role in Grk diffusion without apparently interfering with the regulation of Grk diffusion by EGFR (Fig. 6, Fig. 7F-K). But what could that role be? Grk movement in the extracellular space between the oocyte and the follicular epithelium is complicated by the formation of the vitelline membrane (see above). Grk could either be released into the extracellular space or it could remain associated with the oocyte plasma membrane and localize to its microvilli. We could not distinguish between these alternatives, as immunofluorescent staining is of insufficient resolution and the extracellular space was not well preserved in our immunoelectron microscopy experiments. Others have nevertheless reported the presence of Grk on microvilli (Bokel et al., 2006). GSLs could therefore be important for Grk targeting to microvilli versus flat portions of the membrane. This, however, is unlikely because Grk still activates EGFR in the *brn* mutant (Table 2 and Fig. 6), indicating that it can encounter its receptor. By contrast, what Grk fails to do in the mutant context is to concentrate along the dorsal midline at a distance from its point of secretion. This suggests that GSLs function in the planar transport of Grk along the AP axis, from one oocyte microvillus to the next, a hypothesis supported by the fact that we found the oocyte microvilli to be oriented parallel to the AP axis (S.P., unpublished).

An intriguing property of secreted Grk in the *brn* mutant context is that it is detected by extracellular staining and not conventional immunostaining. In an effort to understand the basis for this, we found that secreted Grk is sensitive to the presence of detergent and to temperature, suggesting that its conformation relies on the presence of GSLs once it reaches the cell surface (see Fig. S1 in the supplementary material). Interestingly, GSLs induce a conformational change in the amyloid β-protein upon its release from the plasma membrane (reviewed by Ariga et al., 2008). It is thus possible that under our experimental conditions, Grk conformation is not fully restored, modifying its ability to diffuse.

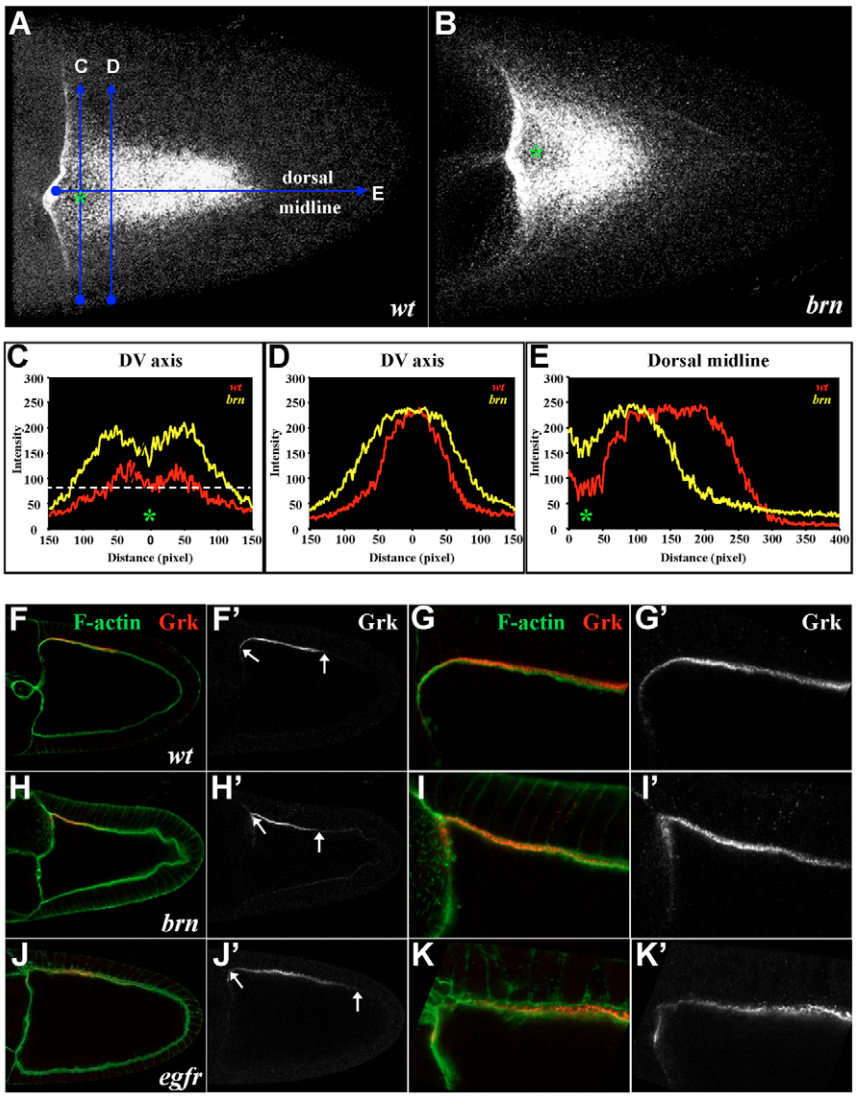

Fig. 7. GSLs shape the extracellular Grk gradient. (**A**,**B**) Stacks of confocal images showing dorsal views (anterior is left) of wild-type (A) and *brn* (B) stage 10a *Drosophila* egg chambers, labeled by immunofluorescence for extracellular Grk. The oocyte nucleus is beneath the asterisk. Under such conditions, Grk is exclusively visualized in the extracellular space. (**C-E**) Plots of average Grk staining intensity along the planes indicated by the arrows in A, from three to five wild-type and *brn* mutant specimens. A value of 0 on the *x*-axis corresponds to the dorsal-most point of planes C,D and to the anterior-most point of plane E. In wild-type egg chambers (A), extracellular Grk (red in C-E) forms a gradient along the DV axis (C,D). Along the AP axis (E), Grk levels are low at the source (asterisk marks the position of the oocyte nucleus, see also C) and rapidly rise to reach a plateau. In *brn* mutant egg chambers (B, yellow in C-E), the shape of the gradient is different in that more Grk accumulates at the source than in the wild type (C), but the length of the plateau is shortened along the AP axis (E). (**F-K'**) Confocal images of stage 10a egg chambers labeled by immunofluorescence for extracellular Grk (red). Enlargements of the DA region of the oocyte and follicular epithelium in G,I,K show the presence of Grk (shown alone in G',I',K') in the extracellular space. In wild-type (F,F') and *brn* mutant (H,H') samples, the extent of extracellular Grk diffusion towards the posterior pole is similar, whereas in *Egfr* mutant samples (J,J'), Grk diffuses further (arrows in F',H',J' delimitate extracellular Grk staining, see text for quantifications). Anterior is to the left, dorsal is up.

In this case, how could the two processes be linked? There is increasing evidence that the spreading of secreted molecules depends on elaborate events involving their multimerization and/or incorporation into higher-order structures such as lipoprotein particles (Gallet et al., 2006; Panakova et al., 2005; Zeng et al., 2001). It is therefore tempting to speculate that a change in secreted Grk conformation that depends on plasma membrane GSLs reflects its packaging into special structures that are required for its efficient transport along microvilli. Since mammalian GSLs can be shed from the plasma membrane and are found circulating with secreted lipoprotein particles (see Clarke, 1981; Lauc and Heffer-Lauc, 2006), GSLs could enhance Grk spreading by delivering it to these particles.

Another, non-mutually exclusive means by which GSLs could affect Grk diffusion is linked to their enrichment in plasma membrane microdomains. Since GSLs can interact with proteins through their oligosaccharide chain, GSLs could bind Grk, or a Grk co-factor, sorting Grk into such domains. It has been reported that Grk is potentially palmitoylated (Miura et al., 2006), and palmitoylation is one of the signals that target proteins to membrane microdomains (reviewed by Pike, 2004). Because Grk recruitment to these domains has not been addressed and because the detection of extracellular Grk by biochemical means in ovaries has so far eluded our attempts (S.P., unpublished), understanding how GSLs regulate Grk diffusion will have to await the generation of better tools.

We thank E. Loeser for great help at the initial stages of this work; D. Xanthakis for excellent technical assistance with the immunoelectron microscopy; N. Perrimon, M. Freeman, J. C. Sisson, S. Roth, T. Schupbach, B. Shilo and C. Ghiglione for sharing reagents; H. H. Wandall, H. Clausen, P. Roth, J. Mathieu, F. Besse, S. Lopez de Quinto, C. Ghiglione and D. St Johnston for very helpful discussions; and A. Gallet, V. Van De Bor and K. Ayers for critical reading of the manuscript. Finally, we thank J.-B. Coutelis for everlasting support and enthusiasm, and for providing the diagrams used to prepare Fig. 1C. This work was supported by the Ligue Contre le Cancer, 'équipe labélisée 2008' and by ANR-07-BLAN-0071-01. S.P. is the recipient of an ARC postdoctoral fellowship.

Supplementary material

Supplementary material for this article is available at
http://dev.biologists.org/cgi/content/full/136/4/551/DC1

References

Ariga, T., McDonald, M. P. and Yu, R. K. (2008). Role of ganglioside metabolism in the pathogenesis of Alzheimer's disease - a review. *J. Lipid Res.* **49**, 1157-1175.

Bokel, C., Dass, S., Wilsch-Brauninger, M. and Roth, S. (2006). Drosophila Cornichon acts as cargo receptor for ER export of the TGFalpha-like growth factor Gurken. *Development* **133**, 459-470.

Chang, W. L., Liou, W., Pen, H. C., Chou, H. Y., Chang, Y. W., Li, W. H., Chiang, W. and Pai, L. M. (2008). The gradient of Gurken, a long-range morphogen, is directly regulated by Cbl-mediated endocytosis. *Development* **135**, 1923-1933.
Chen, Y. W., Pedersen, J. W., Wandall, H. H., Levery, S. B., Pizette, S., Clausen, H. and Cohen, S. M. (2007). Glycosphingolipids with extended sugar chain have specialized functions in development and behavior of Drosophila. *Dev. Biol.* **306**, 736-749.
Chou, T. B. and Perrimon, N. (1992). Use of a yeast site-specific recombinase to produce female germline chimeras in Drosophila. *Genetics* **131**, 643-653.
Clarke, J. T. (1981). The glycosphingolipids of human plasma lipoproteins. *Can. J. Biochem.* **59**, 412-417.
Clifford, R. and Schupbach, T. (1994). Molecular analysis of the Drosophila EGF receptor homolog reveals that several genetically defined classes of alleles cluster in subdomains of the receptor protein. *Genetics* **137**, 531-550.
Degroote, S., Wolthoorn, J. and van Meer, G. (2004). The cell biology of glycosphingolipids. *Semin. Cell Dev. Biol.* **15**, 375-387.
Dorman, J. B., James, K. E., Fraser, S. E., Kiehart, D. P. and Berg, C. A. (2004). bullwinkle is required for epithelial morphogenesis during Drosophila oogenesis. *Dev. Biol.* **267**, 320-341.
Duffy, J. B., Harrison, D. A. and Perrimon, N. (1998). Identifying loci required for follicular patterning using directed mosaics. *Development* **125**, 2263-2271.
Gallet, A., Ruel, L., Staccini-Lavenant, L. and Therond, P. P. (2006). Cholesterol modification is necessary for controlled planar long-range activity of Hedgehog in Drosophila epithelia. *Development* **133**, 407-418.
Ghiglione, C., Bach, E. A., Paraiso, Y., Carraway, K. L., 3rd, Noselli, S. and Perrimon, N. (2002). Mechanism of activation of the Drosophila EGF Receptor by the TGFalpha ligand Gurken during oogenesis. *Development* **129**, 175-186.
Goentoro, L. A., Reeves, G. T., Kowal, C. P., Martinelli, L., Schupbach, T. and Shvartsman, S. Y. (2006). Quantifying the Gurken morphogen gradient in Drosophila oogenesis. *Dev. Cell* **11**, 263-272.
Gonzalez-Reyes, A., Elliott, H. and St Johnston, D. (1995). Polarization of both major body axes in Drosophila by gurken-torpedo signalling. *Nature* **375**, 654-658.
Goode, S., Wright, D. and Mahowald, A. P. (1992). The neurogenic locus brainiac cooperates with the Drosophila EGF receptor to establish the ovarian follicle and to determine its dorsal-ventral polarity. *Development* **116**, 177-192.
Goode, S., Melnick, M., Chou, T. B. and Perrimon, N. (1996a). The neurogenic genes egghead and brainiac define a novel signaling pathway essential for epithelial morphogenesis during Drosophila oogenesis. *Development* **122**, 3863-3879.
Goode, S., Morgan, M., Liang, Y. P. and Mahowald, A. P. (1996b). Brainiac encodes a novel, putative secreted protein that cooperates with Grk TGF alpha in the genesis of the follicular epithelium. *Dev. Biol.* **178**, 35-50.
Griffitts, J. S., Haslam, S. M., Yang, T., Garczynski, S. F., Mulloy, B., Morris, H., Cremer, P. S., Dell, A., Adang, M. J. and Aroian, R. V. (2005). Glycolipids as receptors for Bacillus thuringiensis crystal toxin. *Science* **307**, 922-925.
Guichard, A., Roark, M., Ronshaugen, M. and Bier, E. (2000). brother of rhomboid, a rhomboid-related gene expressed during early Drosophila oogenesis, promotes EGF-R/MAPK signaling. *Dev. Biol.* **226**, 255-266.
Herpers, B. and Rabouille, C. (2004). mRNA localization and ER-based protein sorting mechanisms dictate the use of transitional endoplasmic reticulum-golgi units involved in gurken transport in Drosophila oocytes. *Mol. Biol. Cell* **15**, 5306-5317.
King, R. C. (1970). *Ovarian Development of Drosophila melanogaster*. New York: Academic Press.
Kolter, T. and Sandhoff, K. (2006). Sphingolipid metabolism diseases. *Biochim. Biophys. Acta* **1758**, 2057-2079.
Lauc, G. and Heffer-Lauc, M. (2006). Shedding and uptake of gangliosides and glycosylphosphatidylinositol-anchored proteins. *Biochim. Biophys. Acta* **1760**, 584-602.
Lisman, Q., Pomorski, T., Vogelzangs, C., Urli-Stam, D., de Cocq van Delwijnen, W. and Holthuis, J. C. (2004). Protein sorting in the late Golgi of Saccharomyces cerevisiae does not require mannosylated sphingolipids. *J. Biol. Chem.* **279**, 1020-1029.
Miljan, E. A., Meuillet, E. J., Mania-Farnell, B., George, D., Yamamoto, H., Simon, H. G. and Bremer, E. G. (2002). Interaction of the extracellular domain of the epidermal growth factor receptor with gangliosides. *J. Biol. Chem.* **277**, 10108-10113.
Miura, G. I., Buglino, J., Alvarado, D., Lemmon, M. A., Resh, M. D. and Treisman, J. E. (2006). Palmitoylation of the EGFR ligand Spitz by Rasp increases Spitz activity by restricting its diffusion. *Dev. Cell* **10**, 167-176.
Neuman-Silberberg, F. S. and Schupbach, T. (1993). The Drosophila dorsoventral patterning gene gurken produces a dorsally localized RNA and encodes a TGF alpha-like protein. *Cell* **75**, 165-174.
Neuman-Silberberg, F. S. and Schupbach, T. (1994). Dorsoventral axis formation in Drosophila depends on the correct dosage of the gene gurken. *Development* **120**, 2457-2463.
Nilson, L. A. and Schupbach, T. (1999). EGF receptor signaling in Drosophila oogenesis. *Curr. Top. Dev. Biol.* **44**, 203-243.
Panakova, D., Sprong, H., Marois, E., Thiele, C. and Eaton, S. (2005). Lipoprotein particles are required for Hedgehog and Wingless signalling. *Nature* **435**, 58-65.
Peri, F., Bokel, C. and Roth, S. (1999). Local Gurken signaling and dynamic MAPK activation during Drosophila oogenesis. *Mech. Dev.* **81**, 75-88.
Peri, F., Technau, M. and Roth, S. (2002). Mechanisms of Gurken-dependent pipe regulation and the robustness of dorsoventral patterning in Drosophila. *Development* **129**, 2965-2975.
Pike, L. J. (2004). Lipid rafts: heterogeneity on the high seas. *Biochem. J.* **378**, 281-292.
Queenan, A. M., Ghabrial, A. and Schupbach, T. (1997). Ectopic activation of torpedo/Egfr, a Drosophila receptor tyrosine kinase, dorsalizes both the eggshell and the embryo. *Development* **124**, 3871-3880.
Queenan, A. M., Barcelo, G., Van Buskirk, C. and Schupbach, T. (1999). The transmembrane region of Gurken is not required for biological activity, but is necessary for transport to the oocyte membrane in Drosophila. *Mech. Dev.* **89**, 35-42.
Rorth, P. (1998). Gal4 in the Drosophila female germline. *Mech. Dev.* **78**, 113-118.
Roth, S., Neuman-Silberberg, F. S., Barcelo, G. and Schupbach, T. (1995). cornichon and the EGF receptor signaling process are necessary for both anterior-posterior and dorsal-ventral pattern formation in Drosophila. *Cell* **81**, 967-978.
Ruohola-Baker, H., Grell, E., Chou, T. B., Baker, D., Jan, L. Y. and Jan, Y. N. (1993). Spatially localized rhomboid is required for establishment of the dorsal-ventral axis in Drosophila oogenesis. *Cell* **73**, 953-965.
Sabourdy, F., Kedjouar, B., Sorli, S. C., Colie, S., Milhas, D., Salma, Y. and Levade, T. (2008). Functions of sphingolipid metabolism in mammals-lessons from genetic defects. *Biochim. Biophys. Acta* **1781**, 145-183.
Sapir, A., Schweitzer, R. and Shilo, B. Z. (1998). Sequential activation of the EGF receptor pathway during Drosophila oogenesis establishes the dorsoventral axis. *Development* **125**, 191-200.
Schupbach, T. (1987). Germ line and soma cooperate during oogenesis to establish the dorsoventral pattern of egg shell and embryo in Drosophila melanogaster. *Cell* **49**, 699-707.
Schwientek, T., Keck, B., Levery, S. B., Jensen, M. A., Pedersen, J. W., Wandall, H. H., Stroud, M., Cohen, S. M., Amado, M. and Clausen, H. (2002). The Drosophila gene brainiac encodes a glycosyltransferase putatively involved in glycosphingolipid synthesis. *J. Biol. Chem.* **277**, 32421-32429.
Sen, J., Goltz, J. S., Stevens, L. and Stein, D. (1998). Spatially restricted expression of pipe in the Drosophila egg chamber defines embryonic dorsal-ventral polarity. *Cell* **95**, 471-481.
Seppo, A., Moreland, M., Schweingruber, H. and Tiemeyer, M. (2000). Zwitterionic and acidic glycosphingolipids of the Drosophila melanogaster embryo. *Eur. J. Biochem.* **267**, 3549-3558.
Sillence, D. J. and Platt, F. M. (2004). Glycosphingolipids in endocytic membrane transport. *Semin. Cell Dev. Biol.* **15**, 409-416.
Strigini, M. and Cohen, S. M. (2000). Wingless gradient formation in the Drosophila wing. *Curr. Biol.* **10**, 293-300.
Urban, S., Lee, J. R. and Freeman, M. (2002). A family of Rhomboid intramembrane proteases activates all Drosophila membrane-tethered EGF ligands. *EMBO J.* **21**, 4277-4286.
Vanzo, N. F. and Ephrussi, A. (2002). Oskar anchoring restricts pole plasm formation to the posterior of the Drosophila oocyte. *Development* **129**, 3705-3714.
Wandall, H. H., Pedersen, J. W., Park, C., Levery, S. B., Pizette, S., Cohen, S. M., Schwientek, T. and Clausen, H. (2003). Drosophila egghead encodes a beta 1,4-mannosyltransferase predicted to form the immediate precursor glycosphingolipid substrate for brainiac. *J. Biol. Chem.* **278**, 1411-1414.
Wandall, H. H., Pizette, S., Pedersen, J. W., Eichert, H., Levery, S. B., Mandel, U., Cohen, S. M. and Clausen, H. (2005). Egghead and brainiac are essential for glycosphingolipid biosynthesis in vivo. *J. Biol. Chem.* **280**, 4858-4863.
Wasserman, J. D. and Freeman, M. (1998). An autoregulatory cascade of EGF receptor signaling patterns the Drosophila egg. *Cell* **95**, 355-364.
Yoon, S. J., Nakayama, K., Hikita, T., Handa, K. and Hakomori, S. I. (2006). Epidermal growth factor receptor tyrosine kinase is modulated by GM3 interaction with N-linked GlcNAc termini of the receptor. *Proc. Natl. Acad. Sci. USA* **103**, 18987-18991.
Zeng, X., Goetz, J. A., Suber, L. M., Scott, W. J., Jr, Schreiner, C. M. and Robbins, D. J. (2001). A freely diffusible form of Sonic hedgehog mediates long-range signalling. *Nature* **411**, 716-720.